

## Effect of Ti Doping on the Structure and Performance of $\text{LNi}_{0.75}\text{Co}_{0.25}\text{O}_2$

HE Hui, CHENG Xuan, ZHANG Ying\*, WANG Shu-fen

(Department of Chemistry, Department of Materials Science & Engineering, State Key Laboratory for Physical Chemistry of Solid Surfaces, Xiamen University, Xiamen 361005, Fujian, China)

**Abstract:** In this study, a series of Co-doped compounds with the formula of  $\text{LNi}_{(0.75-x)}\text{Co}_{0.25}\text{Ti}_x\text{O}_2$  ( $x = 0, 0.1, 0.25$ ) was synthesized by using sol-gel method. Their structure, particle size, electrochemical properties were studied by TG, XRD, SEM and electrochemical tests. It was shown that the structure of materials changed from a hexagonal layered structure to a cubic structure as the  $x$  value increased. In particular, a mixture of hexagonal and cubic structure was presented at  $x = 0.25$ . The electrochemical performance of the materials depended strongly on the amount of Ti doping. Possible effects on the structure and performance of  $\text{LNi}_{(0.75-x)}\text{Co}_{0.25}\text{Ti}_x\text{O}_2$  due to Ti doping are briefly discussed based upon the experiment and computational results.

**Key words:** Lithium ion batteries, Cathode materials, Ti doping, Electrochemical performance

CLC Number: TM 912.9

Document Code: A

### 1 Introduction

Lithium cobalt oxide has been widely used as a cathode (positive electrode) material for commercial secondary lithium-ion batteries due to its advantages of easy preparation, high voltage, good reversibility, and high theoretical specific capacity. A  $\text{LiCoO}_2$  cathode with a carbon anode to make the first successful Li-ion battery<sup>[1-2]</sup>, which now dominates the lithium battery market. There is a limited availability of cobalt, which causes it to have a high price and also cobalt brings the environment pollution<sup>[2]</sup>. In order to tackle the problems associated with the high cost and system instability of  $\text{LiCoO}_2$ , a method for the preparation of a version of the compound which has improved electrochemical characteristics and cationic substitutions on the cobalt sites has been sought extensively. Of these substituted compounds,  $\text{LNi}_x\text{Co}_{1-x}\text{O}_2$  has been identified as one of the most

attractive materials. The layered  $\text{LNi}_x\text{Co}_{1-x}\text{O}_2$  ( $0 < x < 1$ ) compounds have been studied extensively as cathode materials for lithium batteries<sup>[6-9]</sup>. The poor thermal stability and cyclability of  $\text{LNi}_x\text{Co}_{1-x}\text{O}_2$  ( $0 < x < 1$ ) demand for doping another element, such as Ti, Al, Mg, Fe, Y, Sr, etc.

Among those doping elements tried, Ti is resourceful in the earth and it has small structure changes when lithium ion intercalation and deintercalation. Previous studies<sup>[10-13]</sup> confirmed that doped Ti can make the structure more stable, hence, improve the thermal stability and cyclability. However, previous work only investigated doped Ti with small amount ( $< 10\%$ ). In order to further study the effect of the amount of Ti doping on the structure and performance and understand the role of Ti played in the cathode material of  $\text{LNi}_x\text{Co}_{1-x}\text{O}_2$ , we used sol-gel method to synthesize a series of  $\text{LNi}_{0.75-x}\text{Co}_{0.25}\text{Ti}_x\text{O}_2$  ( $x = 0,$

0.1, 0.25). The structure, morphology, electrochemical performance and electric state of the materials at different  $x$  values both experimentally and by calculation using VASP were examined.

## 2 Experimental

### 2.1 Synthesis of Materials

Three types of  $\text{LNi}_{0.75-x}\text{Co}_{0.25}\text{Ti}_x\text{O}_2$  ( $x=0, 0.1, 0.25$ ) were prepared by sol-gel pretreatment using citric acid as a chelating agent and solid-phase formation. A stoichiometric amount of lithium nitrate ( $\text{LiNO}_3$ ), nickel nitrate ( $\text{Ni(NO}_3)_2 \cdot 6\text{H}_2\text{O}$ ) and cobalt nitrate ( $\text{Co(NO}_3)_2 \cdot 6\text{H}_2\text{O}$ ) was dissolved in absolute ethyl alcohol and mixed with aqueous solution of citric acid. And then a stoichiometric amount of tetrabutyl titanate ( $\text{C}_{16}\text{H}_{36}\text{O}_4\text{Ti}$ ) was added. The resulting solution was stirred at 80 °C for more than 12 h to obtain a clear viscous gel. The gel was dried at an oven at 120 °C

for 12 h.  $\text{LNi}_{0.75-x}\text{Co}_{0.25}\text{Ti}_x\text{O}_2$  ( $x=0, 0.1, 0.25$ ) were calcined at 725 °C for 2 h after precalcining the obtained precursor at 380 °C. During heating and cooling, the variation of the temperature was fixed at 1 °C/min.

### 2.2 Characterization of Materials

The thermal analysis was carried out on a Netzsch STA 400 analyzer with 50 mL/min of flowing air and a heating rate of 10 °C/min in the temperature range of 323 ~ 1273 K using precursors of dry gels. The structures of the materials prepared were characterized by powder X-ray diffraction (XRD), using Philips Panalytical X'pert diffractometer with CuK $\alpha$  radiation operated at 40 kV and 30 mA. The data were collected in the  $2\theta$  range of 10° ~ 90° using a step size of 0.0167° and a counting time of 10 s per step. The morphologies of the materials were obtained by using a scanning electron microscope (LEO 1530 field emission SEM, Oxford Instruments) which was operated at 15 kV. The samples were coated by Au before the SEM observation.

Electrochemical characterization was performed with coin-type cells. The cathode was prepared by mixing an 85:5:10 (w/w) ratio of active material, carbon black, and polyvinylidene fluoride binder, re-

spectively, in *N*-methyl pyrrolidinone. Lithium metal was used as an anode and a polypropylene separator was used to separate the anode and the cathode; 1.0 mol/L  $\text{LiPF}_6$  dissolved in a 1:1 mixture of ethylene carbonate / diethyl carbonate was used as an electrolyte. The charge and discharge cycles were carried out at a 0.1 C-rate over a potential range between 2.7 and 4.4V.

### 2.3 Calculation

All calculations were performed in the generalized gradient approximation (GGA) to density functional theory as implemented in the Vienna Ab Initio Simulation Package (VASP). A plane-wave basis set with a kinetic-energy cutoff of 500 eV was used. The reciprocal space sampling was done with a 4 × 4 × 4  $k$ -point grid for structures containing 4 grids.

## 3 Results and Discussion

Figure 1 shows the TGA-DTG curves of the dry-gel precursors prepared for the precalcination and calcination processes. The symbols  $C_1$ ,  $C_2$  and  $C_3$  in the figure represent  $\text{LNi}_{0.75}\text{Co}_{0.25}\text{O}_2$ ,  $\text{LNi}_{0.65}\text{Co}_{0.25}\text{Ti}_{0.1}\text{O}_2$  and  $\text{LNi}_{0.5}\text{Co}_{0.25}\text{Ti}_{0.25}\text{O}_2$ , respectively. Below 200 °C, all three types of the materials had small peaks, and this weight loss of the precursors could be due to the desorption of superficial and structural water. In the temperature range of 200 ~ 300 °C, a peak occurred due to the decomposition of nitrate and/or the dehydration of metal citrate to aconitate<sup>[14]</sup>. Then a sharp drop in weight appeared between 350 °C and 400 °C, which is attributed to the combustion of aconitate and its complex. There were small changes in the temperature range of 400 ~ 600 °C. When the temperature was higher than 700 °C, a small peak appeared and could be related to the decomposition of carbonate. It is evident that temperature of phase transformation for  $C_1$  was above 650 °C, while the temperature for the phase transformation of  $C_2$  and  $C_3$  were about 600 °C and 500 °C, respectively. Thereby, the thermal stability can be improved by increasing the amount of Ti doping.

Based on the TGA/DTA results given in Fig 1, eight characteristic temperatures, namely, 350 °C,

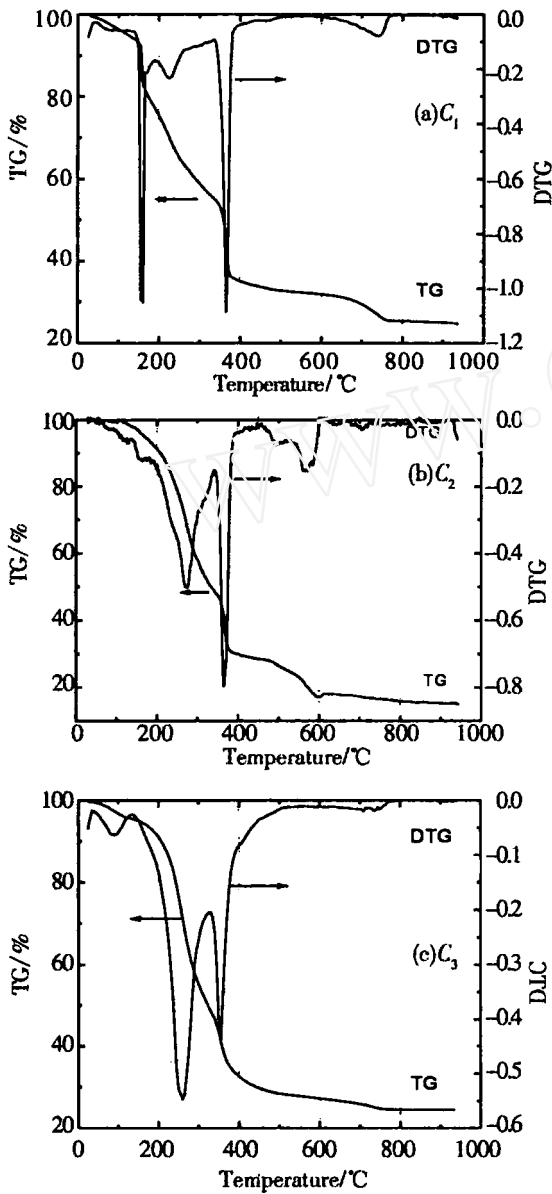


Fig 1 TG-DTG curves of the dry-gel precursor of three different amounts of Ti doped materials

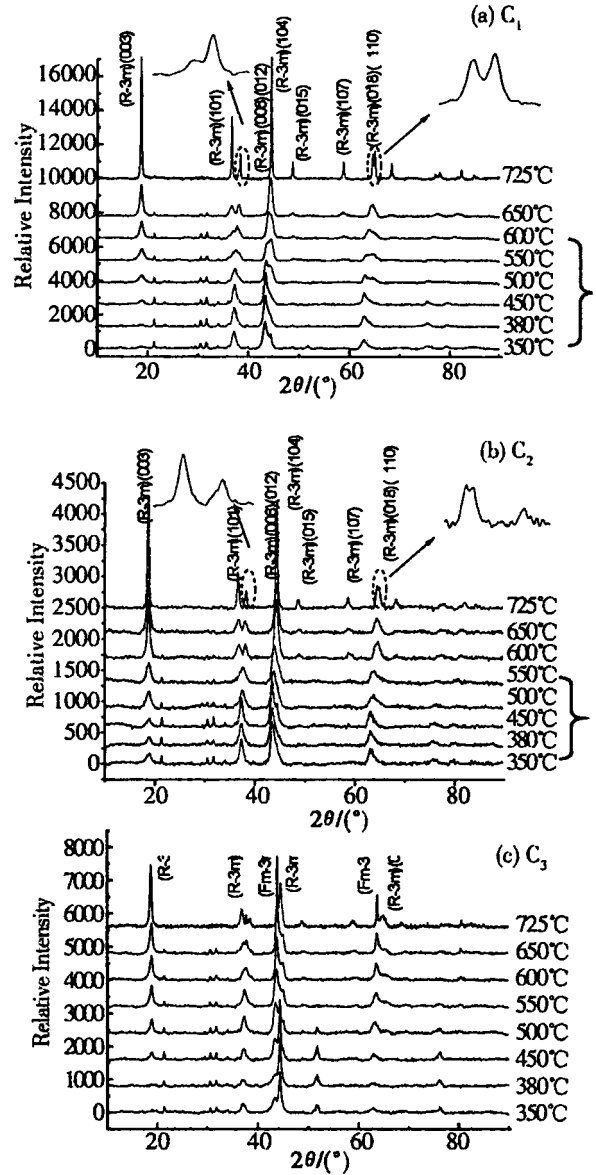


Fig 2 XRD patters of three different amount of Ti doped materials on synthesized at for 2 hours

380 , 400 , 450 , 500 , 550 , 600 , 650 and 725 , were selected and a series of XRD measurements at each temperature kept for 2 h was made ex-situ . Figure 2 shows the XRD patters of  $C_1$  ,  $C_2$  , and  $C_3$  at eight characteristic temperatures raised consequently from 350 to 725 . The precursors were first heated up to each of the selected temperatures and kept constant in the oven for 2 h, and then were analyzed by XRD at room temperature. The XRD patters of  $C_1$  ,  $C_2$  and  $C_3$  kept at 725 are those of finished product . It can be seen from Fig 2a

that  $C_1$  at 725 had the typically hexagonal structure with the space group of R-3m. For hexagonal structure, the relative intensities of XRD lines  $I_{(003)} / I_{(104)}$  or  $I_{(101)} / I_{(006,102)}$  are considered to be indicators of the ordering of lithium and other transition metal cations (Ni and/or Co)<sup>[15]</sup>, and the ordering of the structure can also be evaluated from the XRD spectra with the degree of either (108)/(110) or (006)/(102) peak splitting. All the peaks belong to those of hexagonal structure and no other phases were presented. The value of  $I_{(003)} / I_{(104)}$  is 1.0027 and (108)/(110)

and (006)/(102) are split, indicating an ordered and layered structure. As evident in Fig 2b,  $C_2$  which calcined at 725 also had hexagonal structure with  $I_{(003)}/I_{(104)}$  being 1.027 and the degree of the peak splitting of (006)/(012) and (018)/(110) was better than that of  $C_1$ . That is to say doped Ti can increase the ordering of lithium and other transition metal cations (Ni and/or Co) and can increase the ordering of structure. However, for  $C_3$  at 725 (Fig 2c), two phases, cubic structure and hexagonal structure co-existed.

From the whole XRD patterns of  $C_1$ , it can be seen the courses of phase transformation from cubic structure to hexagon structure. In the temperature range of 350 ~ 600, the XRD patterns were similar, and all the peaks were characteristic of the cubic structure, the development of (003) and (104)

peaks with the increase of temperature became apparent. The phase transformation took place above 650 and the hexagonal structure replaced the cubic structure. With the increase of temperature, the intensity of characteristic peaks became stronger and well-defined, the degree of the peak splitting in (006)/(012) and (018)/(110) became significant. For  $C_2$  the hexagonal structure was obtained at above 600, both agreed well with the TGA results. In the case of  $C_3$ , two phases were presented through the whole temperature range. The results in Fig 2 suggested the better defined hexagonal and layered structure can be obtained at  $x = 0.1$ . While two phases are presented with  $x = 0.25$ .

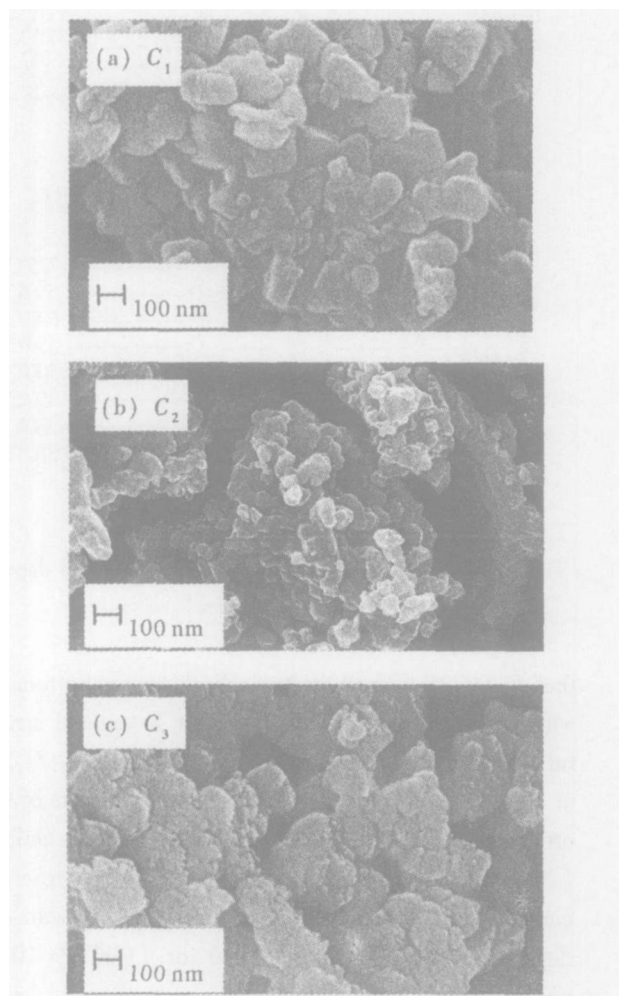


Fig 3 Micrographs of three types of cathode materials synthesized at 725 °C for 2 hours

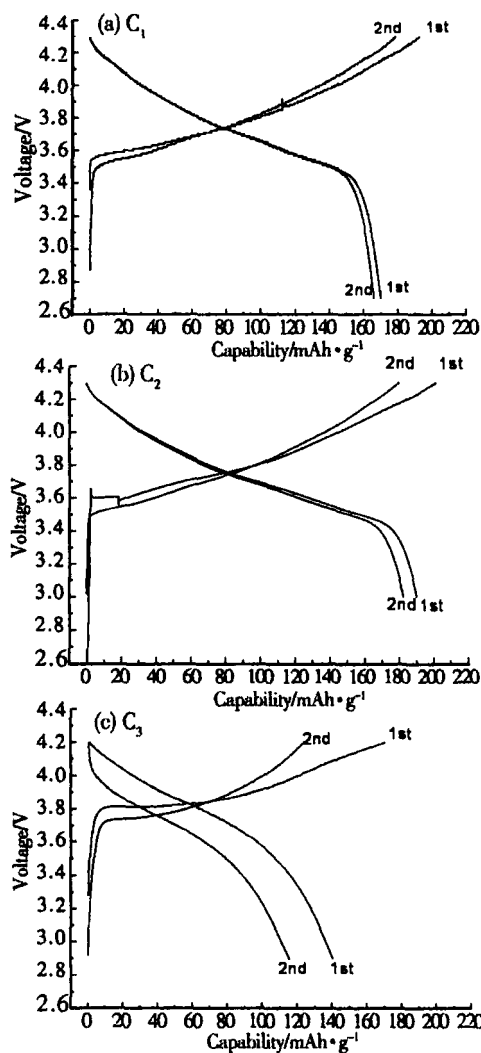


Fig 4 Cyclic discharge curves of the first two cycles of three different amounts of Ti doped materials

Tab 1 Summary of cycling performance from Fig 4

		Material		
		$C_1$	$C_2$	$C_3$
First	Charge capacity / $\text{mAh} \cdot \text{g}^{-1}$	193	201	170
	Discharge capacity / $\text{mAh} \cdot \text{g}^{-1}$	172	190	140
	Loss(%)	12	6	18
Second	Charge capacity / $\text{mAh} \cdot \text{g}^{-1}$	178	181	123
	Discharge capacity / $\text{mAh} \cdot \text{g}^{-1}$	166	179	115

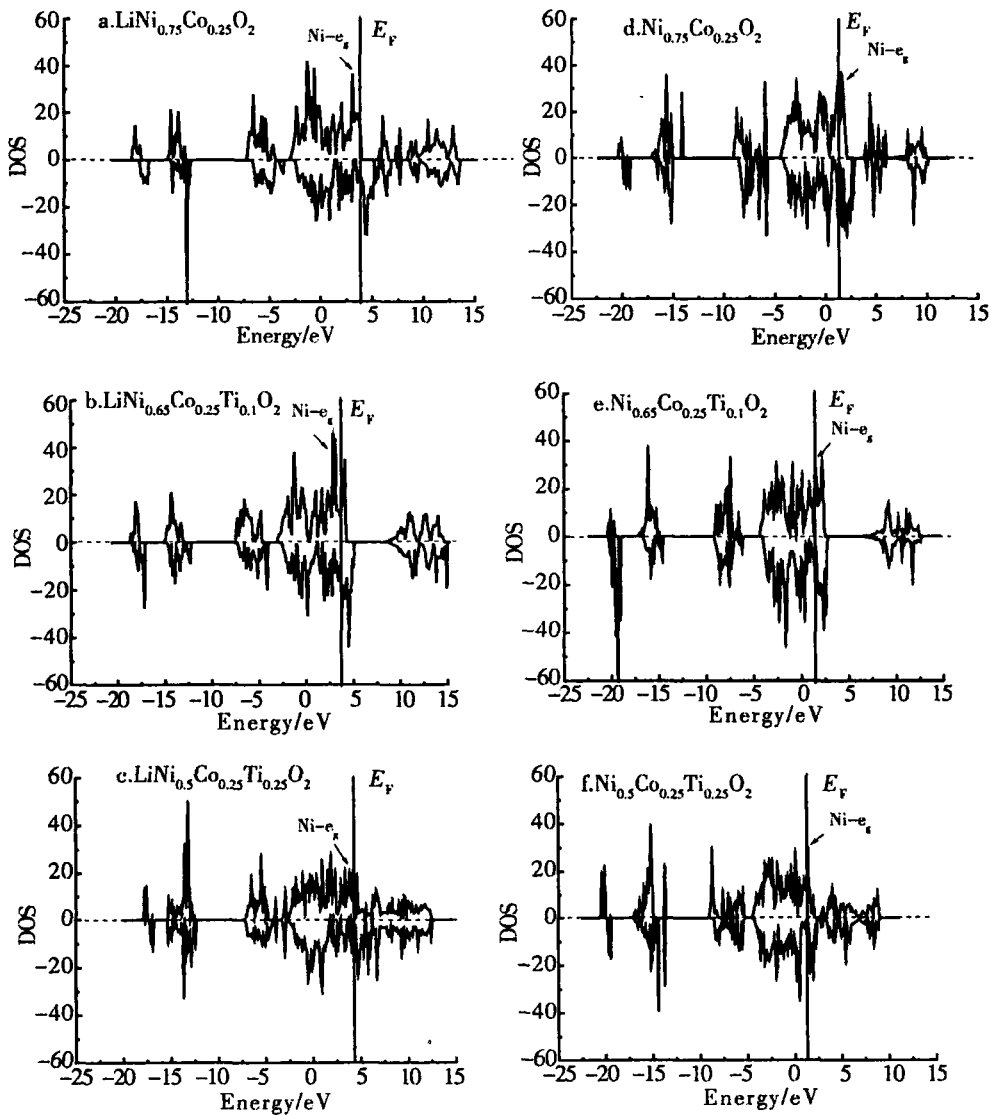


Fig 5 DOS of three different amount of Ti doped materials a) ~ c) lithiation, d) ~ f) delithialization

Figure 3 is the SEM micrographs of  $C_1$ ,  $C_2$ , and  $C_3$  which calcined at  $725^\circ\text{C}$  for 2 h after precalcining

the obtained precursor at  $380^\circ\text{C}$ . It can be seen that the shape of the particles for  $C_1$  and  $C_2$  was regular

with clear edges (Fig 3a and 3b), indicating good crystal structure. The particle sizes for  $C_2$  are smaller and more uniform than those of  $C_1$ . The morphology revealed  $C_3$  indistinct edges of particles and rough surfaces, hence poor structure. The SEM observation is consistent with the XRD results discussed before.

Figure 4 compares the first charge and discharge curves of these three materials. For  $C_1$  and  $C_2$ , they both had plateaus at about 3.6 V, but for  $C_3$ , there was no obvious plateau. The charge/discharge capacities and their losses are summarized in Table 1. It can be seen that for  $C_1$  the first charge capacity was 193 mAh/g and the first cycle loss was 12%. The first charge capacity for  $C_2$  reached 201 mAh/g while which is higher than that of  $C_1$ , the first cycle loss maintained at 6%, suggesting that the cyclability of  $C_2$  is better than that of  $C_1$ . The first charge capacity for  $C_3$  was 23 mAh/g lower and the first cycle loss was 6% higher than those of  $C_1$ , suggesting poor electrochemical performance.

The density of states for  $\text{Li}_y\text{Ni}_{1.75-x}\text{Co}_{0.25}\text{Ti}_x\text{O}_2$  ( $x = 0, 0.1, 0.25$ ) when  $y = 1$  and  $y = 0$  were calculated and the results are provided in Fig 5. When the lithium ion deintercalation occurred, the energy of Fermi ( $E_F$ ) was lower and the  $\text{Ni}-e_g$  orbit moved to a higher level of  $E_F$ , indicating the degree of polarization on  $\text{Ni}-\text{O}$  and  $\text{Co}-\text{O}$  increased, hence, the valence of Ni ion changed from  $+\text{Ni}(\ )$  to  $+\text{Ni}(\ )$ . The doping with small amount of Ti ( $x = 0.1$ ) increased the DOS of  $\text{Ni}-e_g$  (Fig 5b), implying that the valences of Ni are  $+\text{Ni}(\ )$  and  $+\text{Ni}(\ )$  with less  $\text{Ni}^{3+}$  and more  $\text{Ni}^{2+}$ . The presence of  $\text{Ni}^{2+}$  made the structure more stable. However, when  $x = 0.25$ , the DOS of  $\text{Ni}-e_g$  decreased, indicating that the high doping with Ti is detrimental to the structure of material. The calculated results agreed well with the experimental results.

## 4 Conclusion

Three types of materials  $\text{LiNi}_{1.75-x}\text{Co}_{0.25}\text{Ti}_x\text{O}_2$  ( $x$

$= 0, 0.1, 0.25$ ) were prepared by sol-gel method and analyzed by TG, XRD and SEM for the structure and morphology information. The electrochemical performance and electron structure were also examined. The results showed that the thermal stability can be improved by doping Ti. Better defined hexagonal structure can be obtained at  $x = 0.1$  with good electrochemical performance. When  $x = 0.25$ , two phases were presented, which resulted in poor electrochemical performance. The calculation of the density of states revealed the change of Ni ion valence during delithiation.

## References:

- [1] Palacin M R, Chabre Y. On the origin of the 3.3 and 4.5 V steps observed in  $\text{LiMn}_2\text{O}_4$ -based spinels [J]. *J. Electrochem. Soc.*, 2000, 147: 845 ~ 853.
- [2] Peng Z S, Wan C R, Jiang C Y, et al. Synthesis by sol-gel process and characterization of  $\text{LiCoO}_2$  cathode materials [J]. *J. Power Sources*, 1998, 72: 215 ~ 220.
- [3] Brousseau M, Biensan P, Simon B. Lithium insertion into host materials: the key to success for Li ion batteries [J]. *Electrochim. Acta*, 1999, 45: 3 ~ 22.
- [4] Ohzuku T, Ueda A. Phenomenological expression of solid-state redox potentials of  $\text{LiCoO}_2$ ,  $\text{LiCo}_{1/2}\text{Ni}_{1/2}\text{O}_2$ , and  $\text{LiNiO}_2$  insertion electrodes [J]. *J. Electrochem. Soc.*, 1997, 144: 2780 ~ 2785.
- [5] Delmas C, Menetrier M, Croguennec L, et al. An overview of the  $\text{Li}(\text{Ni},\text{M})\text{O}_2$  systems: syntheses, structures and properties [J]. *Electrochim. Acta*, 1999, 45: 243 ~ 253.
- [6] Banov B, Bourilkov J, Mladenov M. Cobalt stabilized layered lithium-nickel oxides, cathodes in lithium rechargeable cells [J]. *J. Power Sources*, 1995, 54: 268 ~ 270.
- [7] Caurat D, Baffier N, Carcia B. Synthesis by a soft chemistry route and characterization of  $\text{LiNi}_x\text{Co}_{1-x}\text{O}_2$  ( $0 < x < 1$ ) cathode materials [J]. *Solid State Ionics*, 1996, 91: 45 ~ 54.
- [8] Alcantara R, Lavela P, Tirado J L. Changes in struc-

- ture and cathode performance with composition and preparation temperature of lithium cobalt nickel oxide [J]. J. Electrochem. Soc., 1998, 145: 730 ~ 736
- [9] Ritchie A G, Giva C O, Lee J C. Future cathode materials for lithium rechargeable batteries [J]. J. Power Sources, 1999, 80: 98 ~ 102
- [10] Jae Woo Joeng, Seong-Gu Kang. Structural and electrochemical properties of  $\text{LNi}_y\text{Ti}_{1-y}\text{O}_2$  prepared by a wet process [J]. J. Power Sources, 2003, 123: 75 ~ 78
- [11] Decheng Li, Takahisa Muta, Hideyuki Noguchi. Electrochemical characteristics of  $\text{LNi}_{0.5}\text{Mn}_{0.5-x}\text{Ti}_x\text{O}_2$  prepared by solid state method [J]. J. Power Sources, 2004, 135: 262 ~ 266
- [12] Kim J H, Myung S T, Yoon C S, et al. Effect of Ti substitution for Mn on the structure of  $\text{LNi}_{0.5}\text{Mn}_{0.5-x}\text{Ti}_x\text{O}_4$  and their electrochemical properties as lithium insertion material [J]. J. Electrochem. Soc., 2004, 151 (11): A1911 ~ A1918
- [13] Molenda J, Wilk P, Marzec J. Transport properties of the  $\text{LNi}_{1-y}\text{Co}_y\text{O}_2$  system [J]. Solid State Ionics, 1999, 119: 19 ~ 22
- [14] Song M Y, Lee R. Synthesis by sol-gel method and electrochemical properties of  $\text{LiNO}_2$  cathode material for lithium secondary battery [J]. J. Power Sources, 2002, 111: 97 ~ 103
- [15] Morales J, Perez-Vicente C, Tirado J L. Cation distribution and chemical deintercalation of  $\text{Li}_{1-x}\text{Ni}_{1+x}\text{O}_2$  [J]. Mater Res Bull, 1990, 25: 623 ~ 630

## 钛掺杂对 $\text{LNi}_{0.75}\text{Co}_{0.25}\text{O}_2$ 结构与性能的影响

贺 慧,程 璇,张 颖\*,王淑芬

(厦门大学化学系,材料科学与工程系,固体表面物理化学国家重点实验室,福建 厦门 361005)

**摘要:** 应用溶胶-凝胶法合成  $\text{LNi}_{(0.75-x)}\text{Co}_{0.25}\text{Ti}_x\text{O}_2$  ( $x=0, 0.1, 0.25$ ) 系列正极材料,其结构、形貌、粒度、电化学性能由 TG、XRD、SEM 和电池充放电测试表征研究表明,材料的电化学性能与钛掺杂量密切相关.在钴含量不变的情况下,随着 Ti 含量 ( $x$ ) 的增加,材料由六方层状结构逐渐向立方结构转变, $x=0.25$  时,出现了立方相与六方相共存.根据实验和理论计算结果简要讨论了钛掺杂对正极材料  $\text{LNi}_{0.75}\text{Co}_{0.25}\text{O}_2$  结构和电化学性能的影响.

**关键词:** 锂离子电池;正极材料;钛掺杂;电化学性能